Phase transitions and spin relaxation in La0.95Sr0.05MnO3

B. I. Kochelaev, E. Shilova, Joachim Deisenhofer, Hans-Albrecht Krug von Nidda, Alois Loidl, A. A. Mukhin, A. M. Balbashov

Angaben zur Veröffentlichung / Publication details:

Kochelaev, B. I., E. Shilova, Joachim Deisenhofer, Hans-Albrecht Krug von Nidda, Alois Loidl, A. A. Mukhin, and A. M. Balbashov. 2003. "Phase transitions and spin relaxation in La0.95Sr0.05MnO3." *Modern Physics Letters B* 17 (10n12): 459–67. https://doi.org/10.1142/S0217984903005482.

PHASE TRANSITIONS AND SPIN RELAXATION IN $La_{0.95}Sr_{0.05}MnO_3$

B. I. KOCHELAEV* and E. SHILOVA†

Kazan State University, Kazan, 400008, Russia
**Boris.Kochelaev@ksu.ru*
†Helen.Shilova@ksu.ru

J. DEISENHOFER, H.-A. KRUG VON NIDDA and A. LOIDL

Experimentalphysik V, Center for Electronic Correlations and Magnetism, Institute for Physics, Augsburg University, D-86135 Augsburg, Germany

A. A. MUKHIN

Institut of General Physics, Russian Academy of Sciences, Moscow, 11794, Russia

A. M. BALBASHOV

Moscow Power Engineering Institute, Moscow, 105835, Russia

We present a model calculation of the paramagnetic-resonance linewidth in $La_{0.95}Sr_{0.05}MnO_3$. Both the temperature and the angular dependencies can be described by contributions from the crystal field due to the cooperative Jahn–Teller transition.

1. Introduction

The interplay between spin and orbital degrees of freedom in $La_{1-x}Sr_xMnO_3$ is the key to understand the complex phase diagram[1–3] of the system and is subject to intense theoretical studies.[4,5] The orbital order (OO) due to the cooperative Jahn–Teller (JT) effect of Mn^{3+}, which characterizes the orthorhombic O' phase, disappears on increasing temperature at the transiton to the weakly distorted orthorhombic O phase at $T_{\rm JT} \approx 750$ K for a Sr concentration $x = 0$. With increasing of doping the JT distorted phase is suppressed and vanishes near $x = 0.2$, which turns out to be a ferromagnetic metal. Experimentally, the JT transition has been investigated by resonant X-ray scattering[6] and by neutron diffraction.[7] Moreover, several electron spin resonance (ESR) investigations report anomalies at the JT transition,[8–12] and an anisotropy of the linewidth in the O' phase.[12,13] This anisotropy has been attributed to contributions of the crystal field (CF) and Dzyaloshinsky–Moriya (DM) interaction in a previous publication.[14] Here we present a consistent theoretical description of both the angular and temperature dependencies of the linewidth for $La_{0.95}Sr_{0.05}MnO_3$.

2. Temperature Dependence of the Linewidth near the Cooperative Jahn–Teller Transition

Paramagnetic resonance of a strongly exchange coupled spin system like $LaMnO_3$ can be described using the formalism developed by Anderson and Weiss[15] and Kubo and Tomita.[16] Our system can be represented by the Hamiltonian

$$\mathcal{H} = -\sum_{i,j} J_{ij}\mathbf{S}_i\mathbf{S}_j + \mu_B \sum_i \mathbf{HgS}_i + \mathcal{H}_{\text{int}} \,. \tag{1}$$

The first term denotes the isotropic superexchange interaction J_{ij} between neighboring spins $\mathbf{S}_i$ and $\mathbf{S}_j$. For $LaMnO_3$, this is reduced to a ferromagnetic $J_{ij} = J_{ac} > 0$ for nearest neighbors within the ac-plane and an antiferromagnetic $J_{ij} = J_b < 0$ for nearest neighbors along the b-axis. To simplify our model we put $J_{ij} = 0$ for all other pairs. The second contribution is the Zeeman energy of the spins in an external magnetic field $\mathbf{H}$. The gyromagnetic tensor $\mathbf{g}$ for Mn^{3+} is only weakly anisotropic in $LaMnO_3$. The last term $\mathcal{H}_{\text{int}}$ includes any contribution, which does not conserve the total spin, like CF, DM interaction, anisotropic exchange, and dipole-dipole interactions. These interactions yield a splitting or broadening of the paramagnetic resonance spectrum. But the strong isotropic exchange averages their influence, resulting in a single exchange-narrowed resonance line. To determine its linewidth $\Delta H = \hbar\Gamma/(g\mu_{\text{B}})$ (half width at half maximum), one has to consider the transverse spin-relaxation rate[17]:

$$\Gamma = \frac{1}{2\hbar^2}\int_{-\infty}^{\infty} d(t-t')\mathcal{K}(t-t') \,. \tag{2}$$

Here the correlation function $\mathcal{K}(t-t')$ of deviations from the Larmor frequency, which are modulated by the isotropic exchange interaction, is given by

$$\mathcal{K}(t-t') = -\frac{\langle [S^\alpha, \mathcal{H}_{\text{int}}]_t \, [S^\alpha, \mathcal{H}_{\text{int}}]_{t'} \rangle}{\hbar^2 \langle S^\alpha S^\alpha \rangle} \tag{3}$$

with the Cartesian spin components of the total spin S^α ($\alpha = x, y, z$). At equal times $t = t'$ Eq. (3) corresponds to the second moment $\mathcal{K}(0) = M_2$ of the EPR resonance line broadened by the interactions $\mathcal{H}_{\text{int}}$. An assumption of a Gaussian random distribution for the correlation function $\mathcal{K}(t-t') = M_2 \exp(-\pi\omega_{\text{ex}}^2(t-t')^2/4)$ allows to calculate the exchange frequency

$$\omega_{\text{ex}}^2 = \frac{2}{\pi M_2}\frac{\partial}{\partial t}\frac{\partial}{\partial t'}\mathcal{K}(t-t')|_{t=t'} \,. \tag{4}$$

Hence, the relaxation rate Eq. (2) can be expressed as

$$\Gamma = \frac{1}{\hbar^2\sqrt{\pi}}\frac{M_2(T)}{\omega_{\text{ex}}(T)} \,. \tag{5}$$

It is important to point out that generally both the second moment and the exchange frequency are temperature dependent.

The temperature dependence of the linewidth below T_{JT} can be revealed, using an observation of Huber *et al.* [9] that well above the magnetic phase transition the

numerator of the correlation function (Eq. (3)) is temperature independent, besides a possible temperature dependence of the coupling constants in $\mathcal{H}_{\rm int}$. Therefore, this numerator can be evaluated at $T \to \infty$. The equal-time correlation function in the denominator of Eq. (3) is known to be $\langle S^\alpha S^\alpha \rangle = k_{\rm B} T \chi(T)$, where $\chi(T)$ is the static spin susceptibility of the spin system and $k_{\rm B}$ is the Boltzmann constant. Hence, for temperatures $T \gg T_{\rm N}$ the transverse relaxation rate can be written as [9]

$$\Gamma(T) = \frac{C}{T\chi(T)} \Gamma(\infty) \tag{6}$$

with $\Gamma(\infty)$ determined from Eq. (5) at $T \to \infty$ and the Curie constant $C = S(S+1)/3k_{\rm B}$. The exchange frequency for this region of temperatures can be evaluated by the moment method as $\omega_{\rm ex}^2(\infty) = (2/\pi\hbar^2) M_4(\infty)/M_2(\infty)$ and is expected to be isotropic, as Huber *et al.* have shown for this particular case by direct calculations of the moments.[9] This means that far above the magnetic phase transition, the angular dependence of the linewidth on the orientation of the external magnetic field is entirely contained in $M_2(\infty)$.

The Mn^{3+} ion has the $3d^4$ electronic configuration having a ground state ^5D with an orbital moment $L = 2$ and spin $S = 2$. The octahedral electric CF splits this energy level into the orbital triplet Γ_5 and the doublet Γ_3 with the latter as the ground state. The orbital wave functions of the doublet have the symmetry $|2^s\rangle = d_{x^2-y^2}$ and $|0\rangle = d_{z^2}$. Below the structural phase transition $O \to O'$ at $T_{\rm JT}$ the MnO_6 octahedra in $LaMnO_3$ become elongated in the *ac*-plane in the mutual perpendicular directions for the nearest octahedra due to the cooperative JT effect. In addition, all octahedra experience a rhombic distortion of the same type.[24] This type of structure and corresponding *OO* can be understood in terms of anisotropic forces between the quantum objects appearing due to the phonon exchange, which can be reduced to the anisotropic elastic interactions, if to neglect the retardation as was shown by Aminov and Kochelaev.[18] The problem of the retardation was considered later in great details by Orbach and Tachiki[19] and the limit of elastic interactions between different orbitals in cubic crystals by Eremin *et al.*[20] This mechanism of *OO* was recently investigated in great detail by Khomskii and Kugel.[21,22] The mentioned distortions of the octahedra result in the splitting of the ground orbital doublet and give further the spin splittings of the ground state due to the spin-orbit interaction. The effective spin Hamiltonian describing these splittings of the ground state of the Mn at the site $\mathbf{R}_j$ can be presented in the following form:

$$\begin{aligned} \mathcal{H}_{\rm CF}^j = {} & \cos^2(\mathbf{R}_j \mathbf{Q}_{\rm JT}/2) \left\{ D(S_j^x)^2 + E\left[(S_j^y)^2 - (S_j^z)^2\right] \right\} \\ & + \sin^2(\mathbf{R}_j \mathbf{Q}_{\rm JT}/2) \left\{ D(S_j^y)^2 + E\left[(S_j^x)^2 - (S_j^z)^2\right] \right\} \end{aligned} \tag{7}$$

which has to be summarized over all Mn coordinates j. The coordinate system in Eq. (7) is defined by the Mn positions of the original undistorted cubic perovskite and hence x and y axes are rotated by $\pi/4$ around $b \parallel z$ with respect to the standard a and c axes of the orthorhombic unit cell. The JT vector $\mathbf{Q}_{\rm JT} = (\pi/d, \pi/d, 0)$

characterizes the alternating distortion of neighboring MnO_6 octahedra within the ac plane, where d denotes the lattice parameter of the undistorted cubic perovskite structure and resembles the distance between two neighboring Mn sites. The zero-field splitting (ZFS) parameters D and E denote the axial and orthorhombic CF contributions, respectively. For a realistic description of the CF, it is necessary to take into account the rotations of the MnO_6 octahedra, which accompany the orthorhombic distortion. Thereby it is convenient to transform the Hamiltonian Eq. (7) into the orthorhombic coordinate system with the z direction along the b axis and the x direction along the c axis. Starting at the undistorted perovskite structure, the orthorhombic structure results from three consecutive small rotations of the octahedra around $y-z-x$ axes by the angles $\beta-\gamma-\alpha$. In the case of orthorhombic symmetry all of the rotations change the sign for consecutive octahedra except of the rotation γ around the z axis, which remains the same for consecutive ac planes as well as the OO due to the cooperative JT effect. Far above magnetic order in linear approximation with respect to α, β, γ, the rotated Hamiltonian yields the second moment

$$M_2(\infty) = \frac{4S(S+1)-3}{20} D^2 f_{\mathrm{reg}}(\vartheta, \varphi) \tag{8}$$

with the regular angular factor

$$\begin{aligned} f_{\mathrm{reg}}(\vartheta, \varphi) = 0.5\{&[1-3\zeta+2\gamma(1+\zeta)]^2[1-\sin^2(\vartheta)\sin^2(\varphi)] \\ &+ [1-3\zeta-2\gamma(1+\zeta)]^2[1-\sin^2(\vartheta)\cos^2(\varphi)] \\ &+ (1+\zeta)^2[2+3\sin^2(\vartheta)]\}\,. \end{aligned}$$

Here ϑ and φ are the polar and azimuth angles between the external magnetic field and $z(b)$ and $x(c)$ axes respectively. $\zeta = E/D$ denotes the ratio of the ZFS parameters. As one can see from Eq. (8), only the rotation around the $z(b)$ axis contributes to the angular dependence in linear approximation and results in the azimuthal variation of the linewidth. This result is a consequence of the simultanious change of the sign of rotations around the $z(b)$ axis and OO for the consecutive octahedra. The exchange frequency for the temperature region under consideration can be estimated using the moments calculated by Huber *et al.*[9] as

$$\omega_{\mathrm{ex}}(\infty) = \frac{4}{\hbar}\sqrt{\frac{6}{\pi}}\sqrt{S(S+1)\langle J^2\rangle} \tag{9}$$

with the averaged exchange integral $\langle J^2\rangle = (2J_{ac}^2 + J_b^2)/3$. Having in mind, that the ZFS parameters are temperature dependent themselves, showing a critical behavior $D = D_0 t^\beta$ and $E = E_0 t^\beta$ with $t \equiv (1 - T/T_{\mathrm{JT}})$ on approaching the structural transition from the O' phase to the O phase, the complete expression for the regular part of the relaxation rate due to the CF reads

$$\Gamma_{\mathrm{reg}} = \frac{C}{T\chi(T)} \Gamma_{\mathrm{CF}}(\infty) \cdot t^{2\beta} f_{\mathrm{reg}}(\vartheta, \varphi) \tag{10}$$

with

$$\Gamma_{\mathrm{CF}}(\infty) = \frac{[4S(S+1)-3]D_0^2}{100\hbar\sqrt{6S(S+1)\langle J^2\rangle}}\,. \tag{11}$$

Inserting the experimental Curie–Weiss (CW) susceptibility $\chi(T) = C/(T-\Theta_{\mathrm{CW}})$, the relaxation contribution Γ_{reg} increases linearly from zero at $T = \Theta_{\mathrm{CW}}$ with increasing temperature, exhibits a negative curvature and is finally suppressed at $T = T_{\mathrm{JT}}$.

3. Critical Behavior near the Magnetic Transition

Now we consider the situation on approaching magnetic order, where the experimental data reveal a critical behavior, which is not included in the regular part of the relaxation rate. At temperatures near T_{N} the local-site spin variables are not suitable any more for the description of the system and we perform a transformation into the wave-vector ($\mathbf{q}$) representation. The straightforward calculation of the second moment yields — after Fourier transformation — a sum over four-spin correlation functions. Having in mind that the system is magnetically isotropic in the paramagnetic regime, we truncate the four spin correlation functions into two spin correlation functions. The result contains the sum of products of pair-correlation functions of the type $\langle S^\alpha_{\mathbf{q}} S^\alpha_{-\mathbf{q}}\rangle^2$ and $\langle S^\alpha_{\mathbf{q}} S^\alpha_{-\mathbf{q}}\rangle\langle S^\alpha_{-\mathbf{q}-\mathbf{Q}_{\mathrm{JT}}} S^\alpha_{\mathbf{q}+\mathbf{Q}_{\mathrm{JT}}}\rangle$. In order to obtain the temperature dependence of these correlation functions, we take into account the AFM coupling along the $z(b)$ direction between the ferromagnetically correlated ac planes represented by the AFM wave vector $\mathbf{Q}_{\mathrm{M}} = (0, 0, \pi/a)$. Using the fluctuation-dissipation theorem in the limit $t \to 0$ and $k_{\mathrm{B}}T/\hbar \gg \omega$, the static correlation functions are given via the Kramers-Kronig relation as

$$\left\langle S^\alpha_{\mathbf{q}} S^\alpha_{-\mathbf{q}}\right\rangle = k_{\mathrm{B}} T \chi(\mathbf{q})\,. \tag{12}$$

A particular case of this relation for $\mathbf{q} = 0$ was quoted above. The Random-Phase Approximation yields for the static spin susceptibility $\chi(\mathbf{q}) = \chi_0/(1 - J(\mathbf{q})\chi_0)$, where $\chi_0 = C/T$ denotes the bare Curie susceptibility. The Fourier transform of the exchange integral $J(\mathbf{q})$ reads

$$J(\mathbf{q}) = 2\left(J_{ac}\cos q_x a + J_{ac}\cos q_y a - |J_b|\cos q_z a\right) \tag{13}$$

with $J_{ac} > 0$ and $J_b < 0$ corresponding to the assumed Heisenberg exchange. Thus, the Néel temperature can be written as $T_{\mathrm{N}} = 2C(2J_{ac} + |J_b|)$. Then expanding $J(\mathbf{Q}_{\mathrm{M}}) - J(\mathbf{q})$ to the second order near $\mathbf{Q}_{\mathrm{M}}$ and assuming $|J_b| = |J_{ac}|$ yields for the two-spin correlation (Eq. (12)):

$$\left\langle S^\alpha_{\mathbf{q}} S^\alpha_{-\mathbf{q}}\right\rangle = \frac{6Ck_{\mathrm{B}}T}{T_{\mathrm{N}}}\left(\frac{\xi}{a}\right)^2 \frac{1}{1+(\xi q)^2}\,, \tag{14}$$

where $(a/\xi)^2 = 6(T - T_{\mathrm{N}})/T_{\mathrm{N}}$ and ξ denotes the magnetic correlation length. At temperatures near T_{N} summation over $\mathbf{q}$ gives

$$\frac{1}{N}\sum_{\mathbf{q}}\left\langle S^\alpha_{\mathbf{q}} S^\alpha_{-\mathbf{q}}\right\rangle^2 = \frac{9(Ck_{\mathrm{B}})^2}{2\pi}\frac{\xi}{a}\,. \tag{15}$$

Thus these terms exhibit a critical behavior. Contrary the other product $\langle S^{\alpha}_{\mathbf{q}} S^{\alpha}_{-\mathbf{q}} \rangle \langle S^{\alpha}_{-\mathbf{q}-\mathbf{Q}_{\mathrm{JT}}} S^{\alpha}_{\mathbf{q}+\mathbf{Q}_{\mathrm{JT}}} \rangle$ gives the regular temperature dependence, which is included in the contribution calculated above. A similar analysis shows that the exchange frequency in this region follows

$$\omega_{\mathrm{ex}}(T) \propto \sqrt{\frac{a}{\xi}}\,, \tag{16}$$

reflecting the slowing down of the spin-fluctuation rate and weakening of the exchange narrowing. Finally, the temperature and angular dependence of the divergent contribution to the transverse relaxation rate reads

$$\Gamma_{\mathrm{div}} = \kappa \frac{D^2}{J} \frac{C}{T\chi(T)} \left(\frac{\xi}{a}\right)^{3/2} f_{\mathrm{div}}(\vartheta, \varphi) \tag{17}$$

with the divergent angular factor

$$\begin{aligned} f_{\mathrm{div}}(\vartheta, \varphi) = 0.5\{&[1 - 3\zeta + 2\gamma(1+\zeta)]^2 [1 - \sin^2(\vartheta)\sin^2(\varphi)] \\ &+ [1 - 3\zeta - 2\gamma(1+\zeta)]^2 [1 - \sin^2(\vartheta)\cos^2(\varphi)]\}\,. \end{aligned}$$

Here κ is a temperature and angular independent dimensionless constant of the order of unity.

4. Comparison with Experimental Data

Now we are prepared to compare our theory with experimental results. According to the previous sections our general fit formula for the temperature and angular dependence of the EPR linewidth can be written as follows

$$\Gamma = \frac{1}{T\chi(T)} \{\Gamma_{\mathrm{DM}}(\infty) + \Gamma_{\mathrm{CF}}(\infty) t^{2\beta} f_{\mathrm{reg}}(\vartheta, \varphi) + \Gamma_{\mathrm{CFD}} t^{2\beta} \tau^{\alpha} f_{\mathrm{div}}(\vartheta, \varphi)\}\,, \tag{18}$$

with $\tau = (T - T_{\mathrm{N}})/T_{\mathrm{N}}$. We admitted a general critical exponent α instead of 0.75 for τ. Here we have taken into account an additional contribution to the linewidth from the anisotropic spin-spin interactions of Dzyaloshinsky-Moriya type, which is represented by the parameter $\Gamma_{\mathrm{DM}}(\infty)$. This contribution is not critical in the whole temperature region and we also neglect its angular dependence. The regular and divergent parts of the crystal field contributions are represented by the parameters $\Gamma_{\mathrm{CF}}(\infty)$ and Γ_{CFD} respectively.

Figure 1 shows the angular dependence of the linewidth in the JT distorted O' phase for $La_{0.95}Sr_{0.05}MnO_3$ at 300 K and 200 K. Figure 2 shows the temperature dependence for the external magnetic field applied along the crystallographic a axis, together with the different theoretical contributions. The data were taken from our previous publication[12] and the corresponding fit curves (solid lines) were obtained with Eq. (18). We used the observed transition temperatures $T_{\mathrm{N}} = 140$ K and $T_{\mathrm{JT}} = 600$ K and $\Theta_{\mathrm{CW}} = 111$ K as fixed parameters in agreement with susceptibility measurements.[3] The rotation angle was taken as $\gamma = 0.23$, which was determined for $LaMnO_3$ by Huang *et al.*[24] The fitting of the data yields the following parameter

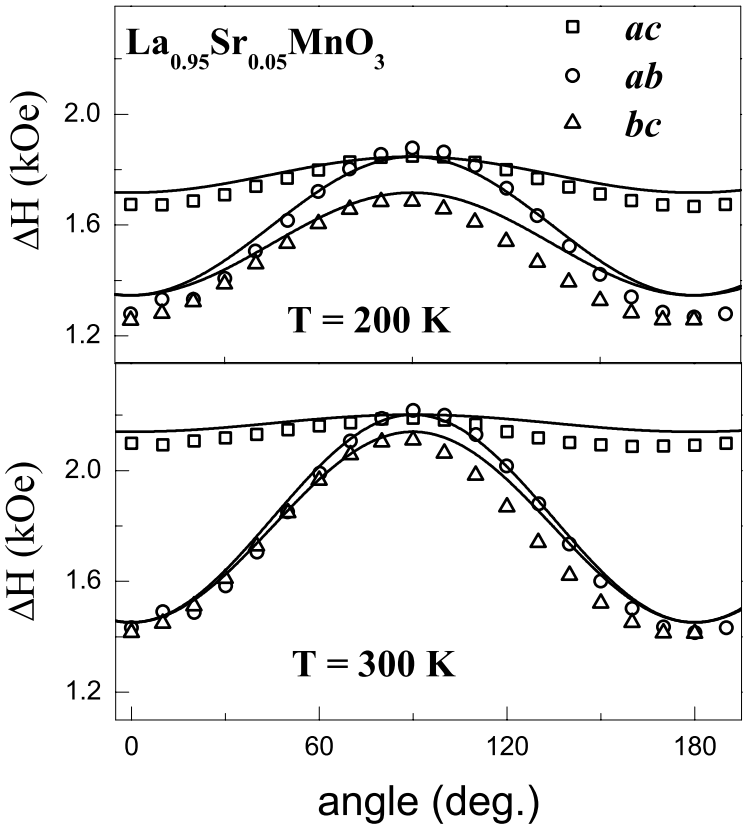

Fig. 1. Angular dependence of ESR linewidth ΔH in $La_{0.95}Sr_{0.05}MnO_3$. The solid lines represent fit curves with the parameters given in the text.

values: $\Gamma_{DM}(\infty) = 1$ kOe; $\Gamma_{CF}(\infty) = 0.57$ kOe; $\zeta = 0.37$; $\Gamma_{CFD} = 10$ kOe; $\beta = 0.16$; $\alpha = 1.8$; $\gamma = 0.23$. One can see that the predicted difference of the angular dependence between the *ab* and *bc* planes sufficiently increases at 200 K due to the divergent contribution because of approaching to the magnetic phase transition in agreement with the experimental data. However, the fitted critical magnetic exponent α is larger than the theoretical value. We were able, also, to reveal the critical exponent of the cooperative JT phase transition $\beta = 0.16$. We would like to point out that both the angular and the temperature dependence are described with the same set of parameters. Only the angular dependence shows an all over shift of 100 Oe because the data were obtained at another crystal with slightly different stoichiometry.

Summarizing, we could describe both the temperature and angular dependence of the linewidth in the JT-distorted phase by the CF and the DM contributions with a single general formula. The main peculiarities of its behavior are well described by the *OO* due to the cooperative JT and magnetic phase transitions.

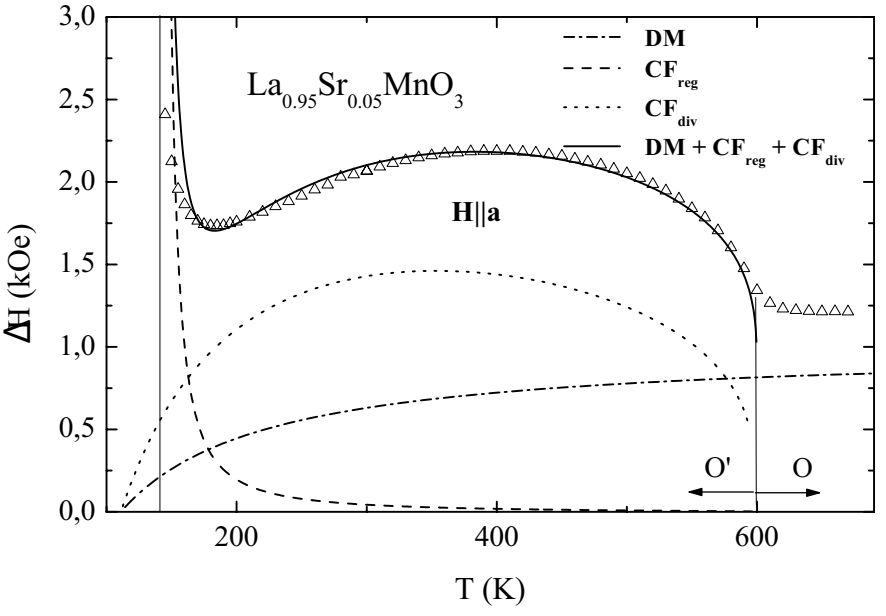

Fig. 2. Temperature dependence of the linewidth and different contributions: the Dzyaloshinsky–Moriya interactions (DM) – dash-dot; the crystal field regular (CFR) – dot; the crystal field divergent (CFD) – dash; the sum of contributions – solid, the fitting parameters are given in the text.

Acknowledgments

This work was supported by the German BMBF under contract No. 13N6917 (EKM) and partly by the Deutsche Forschungsgemeinschaft (DFG) via the Sonderforschungsbereich 484 and DFG-project 436-RUS-113/566. B. I. Kochelaev and E. Shilova were partially supported by INTAS-01-0654 and CRDF via grant REC-007.

References

1. A. Urushibara *et al.*, *Phys. Rev.* **B51**, 14103 (1995).
2. J.-S. Zhou *et al.*, *Phys. Rev. Lett.* **79**, 3234 (1997).
3. M. Paraskevopoulos *et al.*, *J. Phys.: Condens. Matter* **79**, 3993 (2000).
4. E. Dagotto *et al.*, *Phys. Rep.* **344**, 1 (2001).
5. Y. Tokura and N. Nagaosa, *Science* **288**, 1462 (2000).
6. Y. Murakami *et al.*, *Phys. Rev. Lett.* **81**, 582 (1998).
7. J. Rodriguez-Carvajal *et al.*, *Phys. Rev.* **B57**, R3189 (1998).
8. M. Causa *et al.*, *J. Magn. Magn. Mat.* **196-197**, 506 (1999).
9. D. L. Huber *et al.*, *Phys. Rev.* **B60**, 12155 (1999).
10. M. Tovar *et al.*, *Phys. Rev.* **B60**, 10199 (1999).
11. J. Deisenhofer *et al.*, *Phys. Rev.* **B66**, 054414 (2002).
12. V. A. Ivanshin *et al.*, *Phys. Rev.* **B61**, 6213 (2000).
13. G. Alejandro *et al.*, *J. Magn. Magn. Mat.* **226–230**, 2002 (2001); *Physica* **B320**, 26 (2002).

14. J. Deisenhofer *et al.*, *Phys. Rev.* **B65**, 104440 (2002); cond-mat/0108515 (2001).
15. P. W. Anderson and P. R. Weiss, *Rev. Mod. Phys.* **25**, 269 (1953).
16. R. Kubo and K. J. Tomita, *J. Phys. Soc. Japan* **9**, 888 (1954).
17. A. Abragam, *The Principles of Nuclear Magnetism* (Clarendon, Oxford, 1961).
18. L. K. Aminov and B. I. Kochelaev, *Zh. Eksp. Theor. Fiz.* **42**, [*Sov. Phys. JETP* **15**, 903 (1962)].
19. R. Orbach and M. Tachiki, *Phys. Rev.* **158**, 524 (1967)
20. M. V. Eremin, A. Yu. Zavidonov and B. I. Kochelaev, *Zh. Eksp. Theor. Fiz.* **90**, 312 (1986) [*Sov. Phys. JETP* **15**, 903 (1962)].
21. D. I. Khomskii and K. I. Kugel, *Phys. Rev.* **B67**, 134401 (2003).
22. K. I. Kugel and D. I. Khomskii, *Usp. Fiz. Nauk.* **15**, 621 (1982).
23. A. Abragam and B. Bleaney, *Electron Paramagnetic Resonance of Transition Ions* (Clarendon, Oxford, 1970).
24. Q. Huang *et al.*, *Phys. Rev.* **B55**, 14987 (1997).